



香港城市大學
City University of Hong Kong

專業 創新 胸懷全球
Professional · Creative
For The World

CityU Scholars

Ultra-Broadband Mode Filter Based on Phase-Shifted Long-Period Grating

Huang, Quandong; Wang, Wen; Jin, Wei; Chiang, Kin Seng

Published in:

IEEE Photonics Technology Letters

Published: 01/07/2019

Document Version:

Post-print, also known as Accepted Author Manuscript, Peer-reviewed or Author Final version

Publication record in CityU Scholars:

[Go to record](#)

Published version (DOI):

[10.1109/LPT.2019.2917388](https://doi.org/10.1109/LPT.2019.2917388)

Publication details:

Huang, Q., Wang, W., Jin, W., & Chiang, K. S. (2019). Ultra-Broadband Mode Filter Based on Phase-Shifted Long-Period Grating. *IEEE Photonics Technology Letters*, 31(13), 1052-1055. Article 8717989. <https://doi.org/10.1109/LPT.2019.2917388>

Citing this paper

Please note that where the full-text provided on CityU Scholars is the Post-print version (also known as Accepted Author Manuscript, Peer-reviewed or Author Final version), it may differ from the Final Published version. When citing, ensure that you check and use the publisher's definitive version for pagination and other details.

General rights

Copyright for the publications made accessible via the CityU Scholars portal is retained by the author(s) and/or other copyright owners and it is a condition of accessing these publications that users recognise and abide by the legal requirements associated with these rights. Users may not further distribute the material or use it for any profit-making activity or commercial gain.

Publisher permission

Permission for previously published items are in accordance with publisher's copyright policies sourced from the SHERPA RoMEO database. Links to full text versions (either Published or Post-print) are only available if corresponding publishers allow open access.

Take down policy

Contact lbscholars@cityu.edu.hk if you believe that this document breaches copyright and provide us with details. We will remove access to the work immediately and investigate your claim.

© 2019 IEEE. Personal use of this material is permitted. Permission from IEEE must be obtained for all other uses, in any current or future media, including reprinting/republishing this material for advertising or promotional purposes, creating new collective works, for resale or redistribution to servers or lists, or reuse of any copyrighted component of this work in other works.

Huang, Q., Wang, W., Jin, W., & Chiang, K. S. (2019). Ultra-Broadband Mode Filter Based on Phase-Shifted Long-Period Grating. *IEEE Photonics Technology Letters*, 31(13), 1052-1055. [8717989]. <https://doi.org/10.1109/LPT.2019.2917388>.

Ultra-broadband Mode Filter Based on Phase-Shifted Long-Period Grating

Quandong Huang, Wen Wang, Wei Jin, and Kin Seng Chiang, *Member, IEEE*

Abstract—We propose an ultra-broadband mode filter based on the structure of a phase-shifted long-period grating formed along a few-mode waveguide terminated with two linear tapers. To demonstrate the operation principle, we design a mode filter to reject the fundamental mode of a three-mode waveguide that supports the E_{11} , E_{21} , and E_{12} modes. Our typical experimental device fabricated with polymer material, which has a length of 26 mm, provides polarization-insensitive 10-dB rejection of the E_{11} mode against the E_{21} and E_{12} modes with bandwidths of ~190 nm (1440 – 1630 nm) and ~140 nm (1450 – 1590 nm), respectively. The proposed mode filter could serve as a general platform for the development of mode filters and mode-dependent-loss compensators for mode-division-multiplexing applications.

Index Terms—Integrated optics devices, gratings, optical polymer, optical waveguide components.

I. INTRODUCTION

MODE-division multiplexing (MDM), where the spatial modes or mode groups of a few-mode fiber (FMF) carry independent signals, is an emerging technology for overcoming the limited transmission capacity of a single-mode fiber (SMF) [1]–[5]. In an MDM system, mode filters that reject or pass selected spatial modes can find many applications. For example, they can be used to reduce modal crosstalks due to imperfect mode demultiplexing, to select specific modes for routing, or to compensate for the mode-dependent loss in the system. Mode filters in MDM systems play the same role as wavelength filters in current wavelength-division-multiplexing (WDM) systems.

In general, it is easy to filter out high-order modes of an FMF, for example, by using fiber/waveguide tapers, bends, or mode multiplexers [6], but it is difficult to filter out the fundamental mode without affecting the high-order modes. A simple fiber structure based on connecting an SMF between two identical two-mode fibers [7] has been demonstrated to suppress the fundamental mode of the two-mode fiber. Such a device, which has a relatively low mode rejection, could be

used as a mode-dependent-loss compensator [7]. Several fundamental-mode-rejection filters have been demonstrated with planar waveguide structures, such as photonic crystals [8] and cascaded Mach-Zehnder interferometers [9], [10], but these devices do not work for modes that have opposite symmetries in the vertical direction (e.g., the LP_{11b} mode). Wavelength-insensitive mode filters with high mode extinction and flexible mode selectivity have been realized with graphene-embedded polymer waveguides [11], but such filters are highly polarization-sensitive. In this paper, we propose and demonstrate a more powerful waveguide platform for the realization of ultra-broadband mode filters.

Our proposed mode filter is based on the principle of converting the mode of a few-mode waveguide (FMW) to be filtered out to a mode of a sufficiently high order by a long-period grating (LPG), which is then suppressed with integrated waveguide tapers. To achieve ultra-broadband operation, we employ a specially designed phase-shifted LPG [12], [13], which, according to the recent study [13], can provide a bandwidth larger than 100 nm. We have demonstrated the idea with preliminary results at a recent conference [14]. In this paper, we provide details in the design, the fabrication, and the characterization of a fundamental-mode rejection filter for a three-mode waveguide with significantly improved results. Our experimental device fabricated with polymer material, which has a length of 26 mm, provides polarization-insensitive 10-dB rejection of the fundamental mode against the two higher-order modes with bandwidths of ~190 nm and ~140 nm, respectively.

II. OPERATING PRINCIPLE AND DESIGN

Figure 1(a) shows the structure of the proposed mode filter, which consists of three waveguide sections connected by two identical linear tapers (Taper 1 and Taper 2). The waveguides at the two ends support three modes, the E_{11} , E_{21} , and E_{12} modes (which correspond, respectively, to the LP_{01} , LP_{11a} , and LP_{11b} modes of an FMF) and the middle widened section supports an additional mode, the E_{31} mode. A phase-shifted LPG is formed along the middle waveguide to convert the E_{11} mode into the E_{31} mode, which is then blocked by the taper at the output end (Taper 2). As a result, the E_{11} mode launched into the input waveguide is selectively filtered out. The wavelength at which the mode-conversion effect is the strongest, i.e., the resonance wavelength λ_0 , is determined by the phase-matching condition:

Manuscript received xx 2019. This work was supported by the Research Grants Council of the Hong Kong Special Administrative Region, China, under Project CityU 11253316. (*Corresponding author: Kin Seng Chiang.*)

Quandong Huang, Wei Jin, and Kin Seng Chiang are with the Department of Electronic Engineering, City University of Hong Kong, 83 Tat Chee Ave., Kowloon, Hong Kong SAR, China (e-mail: qd.huang@my.cityu.edu.hk; weijin@cityu.edu.hk; eksc@cityu.edu.hk).

Wen Wang is with the School of Optoelectronic Science and Engineering, University of Electronic Science and Technology of China, Chengdu, 610054 China (e-mail: wangwen@std.uestc.edu.cn).

$$\lambda_0 = (N_{11} - N_{31})\Lambda, \quad (1)$$

where N_{11} and N_{31} are the effective indices of the E_{11} and E_{31} modes, respectively, and Λ is the grating period.

In our design, we fix the refractive indices of the core and the cladding of the waveguides at 1.569 and 1.559, respectively, which are the refractive indices of the polymer materials used in our fabrication work. We also fix the height of the cores at $9.0 \mu\text{m}$. We analyze the modes of the waveguides by the full-vector finite-element method with a commercial mode solver (COMSOL). To ensure that the waveguides support the expected numbers of modes, we choose a width of $8.0 \mu\text{m}$ for the cores at the two ends and a width of $14.0 \mu\text{m}$ for the widened core. Each taper has a length of 1 mm . The effective indices of the E_{11} and E_{31} modes supported by the widened waveguide are 1.5669 and 1.5617, respectively, for the TE polarization. With these results, we choose a grating period of $\Lambda = 302 \mu\text{m}$, which, according to Eq. (1), corresponds to a resonance wavelength of 1570 nm .

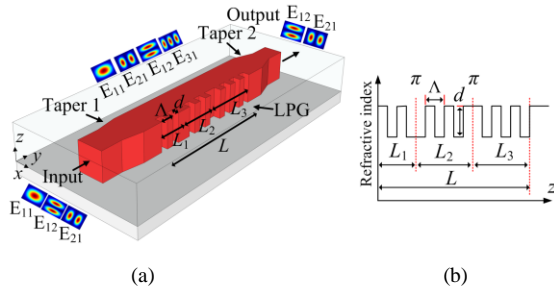


Fig. 1. (a) The proposed ultra-broadband mode filter consists of three waveguide sections connected by two identical linear tapers (Taper 1 and Taper 2) and a phase-shift LPG formed along the middle section, where the waveguide at each end supports the E_{11} , E_{21} , and E_{12} modes and the middle widened section supports an additional mode, the E_{31} mode. (b) Refractive-index profile of a three-section phase-shifted LPG, which consists of three uniform gratings sections of different lengths (L_1 , L_2 , and L_3) with a π -phase shift introduced between two neighbor sections.

Figure 1(b) shows the profile of a three-section phase-shifted LPG used in our study, which consists of three uniform gratings sections of different lengths (L_1 , L_2 , and L_3) with a π -phase shift introduced between two neighbor sections. A three-section phase-shifted LPG has been proven to be sufficient to provide a large bandwidth [13]. To achieve conversion between the E_{11} and E_{31} modes, we use a sidewall grating with a core corrugation depth d , as shown in Fig. 1. The condition for zero transmission of the E_{11} mode at the resonance wavelength obtained from the transfer-matrix method is given by [12]

$$\text{Abs}(-L_1 + L_2 - L_3) = \frac{\pi}{2\kappa} \quad (2)$$

where κ is the coupling coefficient, which is a measure of the overlap integral between the two coupled modes in the grating area [15]. With extensive numerical computation by following the method elaborated elsewhere [13], we can optimize the length distribution and the value of κ required. Here we present our results for a total of 42 grating periods, i.e., $L = L_1 + L_2 + L_3 = 42\Lambda = 12.68 \text{ mm}$, with $L_2 = L/3 = 14\Lambda$ and $L_1 + L_3 = 28\Lambda$. From Eq. (2), we find $\kappa = 372 \text{ m}^{-1}$, which corresponds to a corrugation depth of $d = 1.3 \mu\text{m}$ (for a 50% corrugation duty

cycle) [15]. Figure 2(a) shows the transmission spectra of the E_{11} mode calculated at $\kappa = 372 \text{ m}^{-1}$ for different combinations of L_1 and L_3 by the transfer-matrix method for the TE polarization [12], where the spectrum of a uniform LPG without any phase shifts is also shown for reference. As shown in Fig. 2(a), the length distribution, $L_1 = 6\Lambda$, $L_2 = 14\Lambda$, and $L_3 = 22\Lambda$ gives the broadest bandwidth. The -10 -dB (i.e., 90% conversion) and -15 -dB (i.e., 97% conversion) bandwidths are 142 nm (from 1500 to 1642 nm) and 128 nm (from 1510 to 1638 nm), respectively. Figure 2(b) shows the transmission spectra of the E_{11} mode calculated for different values of the coupling coefficient κ for the length distribution, $L_1 = 6\Lambda$, $L_2 = 14\Lambda$, and $L_3 = 22\Lambda$. As shown in Fig. 2(b), the -20 -dB bandwidth is sensitive to the value of κ . To achieve a -20 -dB bandwidth larger than $\sim 60 \text{ nm}$, the range of the value of κ should be $372 \pm 15 \text{ m}^{-1}$. The -10 -dB and -15 -dB bandwidths, however, are insensitive to the value of κ . The results for the TM polarization are almost the same. The small core-cladding index difference and the broadband nature of the mode filter ensure polarization-insensitive operation.

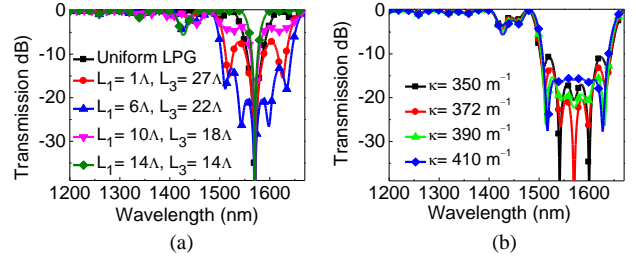


Fig. 2. Transmission spectra of the E_{11} mode for a three-section phase-shifted LPG calculated (a) for different length distributions at $\kappa = 372 \text{ m}^{-1}$ and (b) at different values of κ for the length distribution, $L_1 = 6\Lambda$, $L_2 = 14\Lambda$, and $L_3 = 22\Lambda$, where the transmission spectrum of a uniform LPG is included in (a).

III. DEVICE FABRICATION

We fabricated the mode filter with our in-house microfabrication facilities by following the design parameters presented in the previous section. We chose the polymer materials EpoCore and EpoClad (Micro Resist Technology GmbH) as the core and the cladding material, respectively. The core and the cladding refractive index, measured by a prism coupler (Metricon 2010) at 1536 nm , were 1.569 and 1.559, respectively. The refractive-index difference between the TE and the TM polarization was smaller than 0.001.

The fabrication processes are illustrated in Fig. 3(a). In Step 1, we used a 100-orientated silicon wafer as the substrate and prepared its surface by reactive-ion etching (RIE) to improve its adhesion. In Step 2, EpoClad was spin-coated onto the silicon substrate and cured to form a thick ($>15 \mu\text{m}$) lower cladding. In Step 3, EpoCore was spin-coated onto the lower cladding to form a core layer and, after curing, etched into the desired pattern (including the grating pattern) by the photolithography process with a properly designed mask. The height of the cores was trimmed into the desired value, i.e., $9.0 \mu\text{m}$, by RIE. In Step 4, EpoClad was spin-coated onto the cores and cured to form a thick ($>15 \mu\text{m}$) upper cladding. The total length of the device was 26 mm .

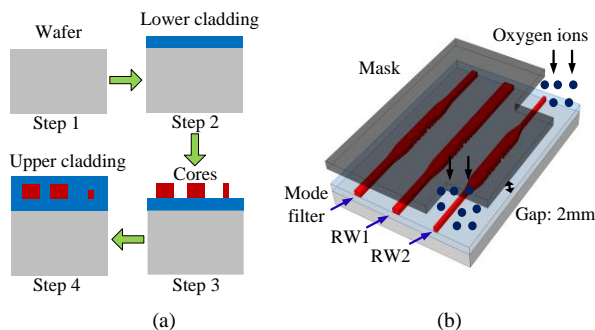


Fig. 3. (a) Steps in the fabrication of the mode filter and the reference waveguide structures and (b) formation of RW2 by tapering the height of the core at both ends.

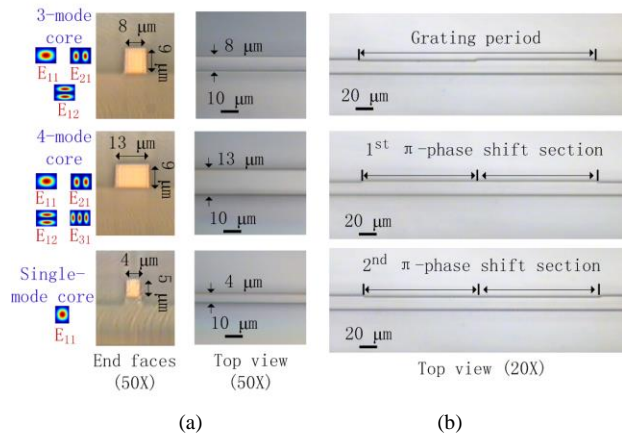


Fig. 4. Microscopic images of (a) the end faces and the surfaces of the three-mode core, the four-mode core, and the single-mode core, which were taken from a fabricated mode filter, RW1, and RW2, respectively, and (b) a grating period and the two π -phase shift sections along the grating.

In addition to the mode filter, we fabricated two reference waveguide structures alongside the device, which are labelled as RW1 and RW2, respectively, as shown in Fig. 3(b). RW1 is identical to the designed mode filter, except that Taper 2 is absent, i.e., the four-mode core is extended to the output end of the device. RW2 is identical to the designed mode filter, except that the four-mode core is tapered into single-mode cores at the two ends by tapering both the width and the height. Tapering of the height of the core was realized by RIE using oxygen ions with a mask placed above the core with a gap distance of 2 mm, as shown in Fig. 3(b) [6]. We also fabricated a number of reference three-core waveguides without tapers and/or gratings for the characterization of taper-induced and grating-induced losses. Figure 4(a) shows microscopic images of the end faces and the surfaces of the three-mode core, the four-mode core, and the single-mode core, which were taken from a fabricated mode filter, RW1, and RW2, respectively. Figure 4(b) shows images of a grating period and the two π -phase shift sections of the grating.

IV. DEVICE CHARACTERIZATION

To characterize the performances of the fabricated devices, we launched the E_{11} , E_{21} , and E_{12} modes into RW1 (the three-mode end) and the mode filter, respectively, with a pigtailed tunable laser (KEYSIGHT) via a lensed fiber and captured the output near-field images of the devices with an

infrared camera. The results for RW1 are shown in Fig. 5(a). With the E_{11} mode launched into RW1, the output mode is the E_{31} mode, which confirms that the LPG functions as an E_{11} - E_{31} mode converter over the C-band. With either the E_{21} mode or the E_{12} mode launched into RW1 (by adjusting the tilt angle and the position of the lensed fiber against the waveguide core with the help of a five-degree micro-positioner), the mode stays. The results for the designed mode filter are shown in Fig. 5(b). With the E_{11} mode launched into the mode filter, there is little output light, which is the result of blocking the E_{31} mode converted from the E_{11} mode by Taper 2. With either the E_{21} mode or the E_{12} mode launched into the mode filter, the mode stays. In fact, no matter how we adjusted the launching condition, we did not observe any significant E_{11} mode at the output of the mode filter, which confirms the function of the device as a fundamental-mode-rejection filter. The mode purity could be estimated with a mode decomposition method [16], [17]. As shown in Fig. 5, the performances of the devices are the same for the TE and TM polarizations.

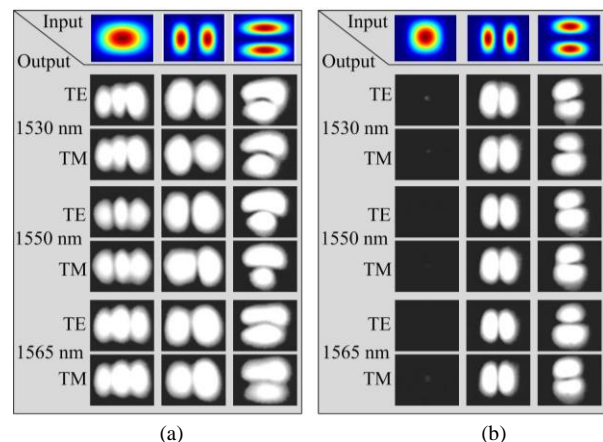


Fig. 5. Output near-field patterns taken from (a) RW1 and (b) the mode filter at different wavelengths in the C-band for the TE and TM polarizations with different modes launched into the devices.

To characterize the bandwidth of the LPG, we launched light from a supercontinuum source (SuperK Compact, KOHERAS) into RW2 and detected the output light with an optical spectrum analyzer (OSA) (AQ6370, Yokogawa). Because the two ends of RW2 support only the E_{11} mode, the use of RW2 guarantees that both the input mode and the output mode are the E_{11} mode. The transmission spectra of the E_{11} mode (normalized to the input power) for the TE and TM polarizations are shown in Fig. 6(a). The wide rejection band shown in Fig. 6(a) is the result of blocking the E_{31} mode converted from the input E_{11} mode by the LPG and, therefore, can be considered as the operation wavelength range of the mode filter. As shown in Fig. 6(a), the -10 -dB ($>90\%$ mode conversion) bandwidth is 197 nm (1438 – 1635 nm), and the -15 -dB ($>97\%$ mode conversion) bandwidth is 97 nm (1473 – 1570 nm). The spectral characteristics of the device are polarization-insensitive.

To measure the effect of the temperature variation on the performance of the fabricated device, we varied the operation temperature of RW2 with an electric heater placed at the button of the device and monitored the change in the

transmission spectrum with the temperature. As shown in Fig. 6(b), the -10 -dB and -15 -dB bandwidths of the device, measured for the TE polarization, decrease slightly from 197 and 97 nm to 182 and 90 nm, respectively, when the temperature increases from 18 to 66 °C. The operation of the device is not particularly sensitive to the ambient temperature, thanks to the broadband characteristics of the grating.

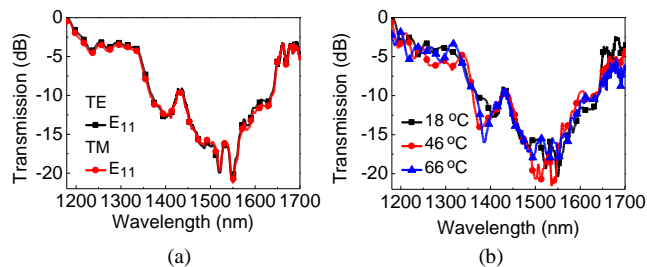


Fig. 6. (a) Normalized transmission spectra of RW2 measured for the TE and TM polarizations and (b) variation of the normalized transmission spectrum of RW2 with the operation temperature measured for the TE polarization.

To measure the modal losses of the mode filter, we excited the E_{21} and E_{12} modes individually with the help of an LPG fiber mode converter written in a two-mode fiber (OFS Fitel, LLC) which had an LP_{01} - LP_{11} mode conversion efficiency higher than 99% at ~ 1550 nm [18]. To avoid the Fresnel reflection, we applied index-matching liquid to the fiber-waveguide interfaces at both ends of the device. The coupling losses of the E_{21} and E_{12} modes between the three-mode waveguide and the two-mode fiber are 1.9 and 1.7 dB, respectively. The insertion losses of the E_{11} , E_{21} , and E_{12} modes measured at 1550 nm (including fiber-waveguide coupling losses) are 29.7, 11.3, and 12.8 dB, respectively, which correspond to an E_{11} -mode rejection ratio of 18.4 dB against the E_{21} mode or 16.9 dB against the E_{12} mode. Without a reliable method to excite the higher-order modes selectively at different wavelengths, we cannot directly measure the loss spectra of the higher-order modes. By assuming that the insertion losses of the higher-order modes are wavelength-insensitive (as confirmed by simulation based on the beam-propagation method), the bandwidths of 10-dB E_{11} -mode rejection against the E_{21} and E_{12} modes are estimated to be ~ 190 nm (1440 – 1630 nm) and ~ 140 nm (1450 – 1590 nm), respectively. The background modal losses could be further reduced by using low-loss polymer materials developed for the C-band [19], and improving the fabrication process.

V. CONCLUSION

We have presented an ultra-broadband fundamental-mode-rejection filter for a three-mode waveguide based on a phase-shifted LPG. Our experimental device fabricated with polymer material provides 10-dB E_{11} -mode rejection against the E_{21} and E_{12} modes with bandwidths of ~ 190 nm (1440 – 1630 nm) and ~ 140 nm (1450 – 1590 nm), respectively. The performance of the device is insensitive to the polarization state of light and the ambient temperature. Our proposed waveguide platform is general and can be applied to the design of a wide range of mode filters and mode-dependent-loss compensators for MDM applications. With our platform,

multiple modes can be filtered out at different degrees with multiple gratings, which could be collocated along the same waveguide. The 3D LPG technology reported recently [20] offers much flexibility in the design of mode converters and can further facilitate the development of this type of grating-based mode filters.

REFERENCES

- [1] R.-J. Essiambre, G. Kramer, P. J. Winzer, G. J. Foschini, and B. Goebel, "Capacity limits of optical fiber networks," *J. Lightw. Technol.*, vol. 28, no. 4, pp. 662–701, Feb. 2010.
- [2] D. J. Richardson, J. M. Fini, and L. E. Nelson, "Space-division multiplexing in optical fibres," *Nat. Photonics*, vol. 7, pp. 354–362, Apr. 2013.
- [3] T. Mizuno and Y. Miyamoto, "High-capacity dense space division multiplexing transmission," *Opt. Fiber Technol.*, vol. 35, pp. 108–117, Feb. 2017.
- [4] Y. Awaji *et al.*, "High-capacity transmission over multi-core fibers," *Opt. Fiber Technol.*, vol. 35, pp. 100–107, Feb. 2017.
- [5] G. Li, N. Bai, N. Zhao, and C. Xia, "Space-division multiplexing: the next frontier in optical communication," *Adv. Opt. Photonics*, vol. 6, no. 4, pp. 413–487, Dec. 2014.
- [6] Q. Huang, Y. Wu, W. Jin, and K. S. Chiang, "Mode multiplexer with cascaded vertical asymmetric waveguide directional couplers," *J. Lightw. Technol.*, vol. 36, no. 14, pp. 2903–2911, July 2018.
- [7] Y. Jung, S. U. Alam, and D. J. Richardson, "All fiber spatial mode selective filter for compensating mode dependent loss in MDM transmission systems," *Proc. The 2015 Optical Fiber Communication Conference*, 2015, W2A.13.
- [8] X. Guan, Y. Ding, and L. H. Frandsen, "Ultra-compact broadband higher order-mode pass filter fabricated in a silicon waveguide for multimode photonics," *Opt. Lett.*, vol. 40, no. 16, pp. 3893–3896, Aug. 2015.
- [9] K. T. Ahmed, H. P. Chan, and B. Li, "Broadband high-order mode pass filter based on mode conversion," *Opt. Lett.*, vol. 42, no. 18, pp. 3686–3689, Sept. 2017.
- [10] C. Sun, W. Wu, Y. Yu, X. Zhang, and G. T. Reed, "Integrated tunable mode filter for a mode-division multiplexing system," *Opt. Lett.*, vol. 43, no. 15, pp. 3658–3661, Aug. 2018.
- [11] Z. Chang and K. S. Chiang, "Ultra-broadband mode filters based on graphene-embedded waveguides," *Opt. Lett.*, vol. 42, no. 19, pp. 3868–3871, Oct. 2017.
- [12] F. Y. M. Chan and K. S. Chiang, "Analysis of apodized phase-shifted long-period fiber gratings," *Opt. Commun.*, vol. 244, pp. 233–243, Jan. 2005.
- [13] W. Wen, W. Jieyun, C. Kaixin, W. Jin, and K. S. Chiang, "Ultra-broadband mode converters based on gratings," *Opt. Express*, vol. 25, no. 13, pp. 14341–14350, Jun. 2017.
- [14] Q. Huang, W. Wang, W. Jin, and K. S. Chiang, "Broadband filtering of the fundamental mode of a few-mode waveguide with a phase-shifted long-period grating," *Proc. Conference on Lasers and Electro-Optics/Pacific Rim*, 2018, Tu3E.5.
- [15] Q. Liu, K. S. Chiang, and V. Rastogi, "Analysis of corrugated long-period waveguide gratings and their polarization dependence," *J. Lightw. Technol.*, vol. 21, no. 12, pp. 3399–3405, Dec. 2003.
- [16] O. Shapira, A. F. Abouraddy, J. D. Joannopoulos, and Y. Fink, "Complete modal decomposition for optical waveguides," *Phys. Rev. Lett.*, vol. 94, no. 14, pp. 143902, Apr. 2005.
- [17] A. M. Velazquez-Benitez *et al.*, "Six mode selective fiber optic spatial multiplexer," *Opt. Lett.*, vol. 40, no. 8, pp. 1663–1666, Apr. 2015.
- [18] J. Dong and K. S. Chiang, "Temperature-insensitive mode converters with CO₂-laser written long-period fiber gratings," *IEEE Photon. Technol. Lett.*, vol. 27, no. 9, pp. 1006–1009, May 2015.
- [19] D. de Felipe *et al.*, "Recent developments in polymer-based photonic components for disruptive capacity upgrade in data centers," *J. Lightw. Technol.* vol. 35, no. 4, pp. 683–689, Feb. 2017.
- [20] W. Jin and K. S. Chiang, "Three-dimensional long-period waveguide gratings for mode-division-multiplexing applications," *Opt. Express*, vol. 26, no. 12, pp. 15289–15299, June 2018.